



Analytic investigation on error of heat flux measurement and data processing for large curvature models in hypersonic shock tunnels



Guilai Han^{*}, Li Qi, Zonglin Jiang

State Key Laboratory of High Temperature Gas Dynamics, Institute of Mechanics, Chinese Academy of Sciences, Beijing, 100190, China
School of Engineering Science, University of Chinese Academy of Sciences, Beijing, 100049, China

ARTICLE INFO

Article history:

Received 31 May 2022
Accepted 17 July 2022
Available online 28 July 2022

Keywords:

Heat flux
Measurement
Data processing
Error
Approximate solution

ABSTRACT

Due to short test time, heat conduction was considered as transient in hypersonic shock tunnels. The heat flux measurement and data processing were operated basing on one-dimensional semi-infinite heat conduction theory. However, for models with local large curvature or small radius, it resulted in significant compression or expansion of space for heat transfer, or lateral heat conduction, which made the hypothesis of one-dimensional unsatisfied and errors. In this paper, approximate solutions for the unsteady heat conduction in cylindrically convex and concave shells were established, and were used for further analysis of the errors, with forms of heating load, location and curvature radius of heated surface taken into consideration.

© 2022 Elsevier Ltd. All rights reserved.

1. Introduction

Hypersonic flights led to severe aerodynamic heating on vehicle surface and even accidents. Hypersonic shock tunnels were usually used to obtain the heat flux at given experimental conditions, simulating flights state [1,2]. Since the test time is as short as tens of milliseconds, the heat flux measurement can be regarded as a transient and time dependent process [3,4]. The one-dimensional semi-infinite heat conduction theory was used to convert the surface temperature into surface heat flux over time, with governing equation and boundary conditions as follows:

$$\frac{\partial T(x, t)}{\partial t} = \frac{k}{\rho c} \frac{\partial^2 T(x, t)}{\partial x^2} \text{ with } \left. \frac{\partial T}{\partial x} \right|_{x=0} = -\frac{q(t)}{k} \text{ and } T|_{x=\infty} = \text{const} \quad (1)$$

With Laplace transformation, the correlation between heat flux and temperature can be obtained

$$q(t) = \frac{\sqrt{\rho c k}}{\sqrt{\pi}} \int_0^t \left. \frac{dT}{d\tau} \right|_{x=0} (t - \tau)^{-\frac{1}{2}} d\tau \quad (2)$$

^{*} Corresponding author at: State Key Laboratory of High Temperature Gas Dynamics, Institute of Mechanics, Chinese Academy of Sciences, Beijing, 100190, China.

E-mail address: hanguilai@imech.ac.cn (G. Han).

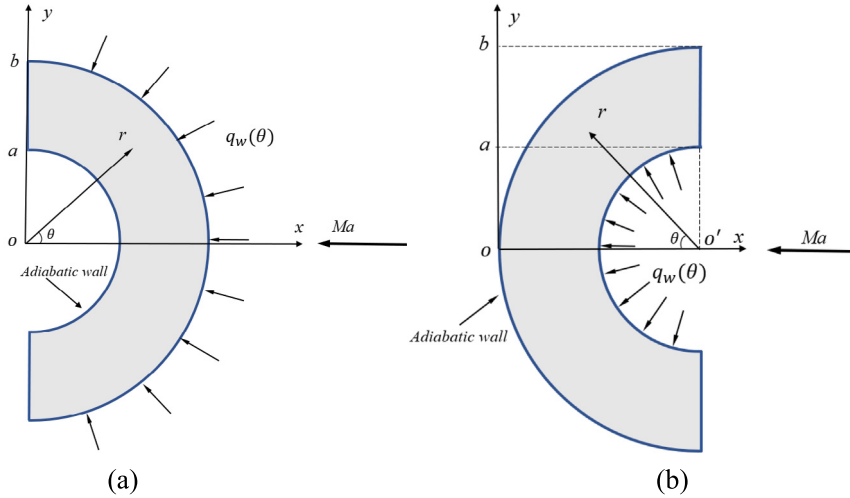


Fig. 1. Schematic of aerodynamic heating on cylindrically convex(a) and concave(b) shells.

with the discrete form for applications usually written as

$$q(t_n) = \frac{\sqrt{\rho c k}}{\sqrt{\pi}} \sum_{i=1}^n \frac{T_i - T_{i-1}}{\sqrt{t_n - t_i} + \sqrt{t_n - t_{i-1}}} \tag{3}$$

One-dimensional theory rests on the basic assumption that curvature is small enough to be neglected. However, there always exist special components of aircraft with large local curvature, such as the leading edge of wing, the junction between wing and fuselage, and airflow compression corners. Large local curvature results in significant two-dimensional or three-dimensional heat conduction [5,6], and obvious error in heat flux processing by Eq. (3). In experiments, the error can always be observed even when we made sensor diameter as small as 0.1 mm.

In this paper, different components of aircraft were simplified into two cylindrical cases, including convex shells for leading edges of wings and rudders and concave shells for joints of wings and bodies. Criteria were set up to truncate the theoretical infinite series solution and form finite approximate solutions, which were validated by numerical simulations. With the approximate solutions, the error analysis under different heat flux loading forms, locations and curvature radius of heat surface were completed.

2. Approximate solutions

As mentioned before, convex shells with heating on $r = b$ and concave shells with heat on $r = a$ were classified and distinguished in Fig. 1. And linear governing equation in cylindrical coordinate system can be written as

$$\frac{1}{\alpha} \frac{\partial T(r, \theta, t)}{\partial t} = \frac{\partial^2 T(r, \theta, t)}{\partial r^2} + \frac{1}{r} \frac{\partial T(r, \theta, t)}{\partial r} + \frac{1}{r^2} \frac{\partial^2 T(r, \theta, t)}{\partial \theta^2} \tag{4}$$

2.1. Exact solution of cylindrically convex shells

For convex case, the boundary and initial conditions can be described as:

$$T_r|_{r=b} = q_w(\theta) \tag{5}$$

$$T_\theta|_{\theta=0} = T_\theta|_{\theta=\pi/2} = 0 \tag{6}$$

$$T|_{r=a} = \text{const} = T_0 \tag{7}$$

$$T|_{t=0} = \text{const} = T_0 \tag{8}$$

For transient process, the heat conduction was assumed not to affect the wall $r = a$. Hence, to simplify the homogenization, Eq. (7) can be replaced with the zero gradient condition $T_r|_{r=a} = 0$.

Basing on superposition principle, general solution can be found in textbooks and expressed as

$$T(r, \theta, t) = V(r, \theta) + W(r, \theta, t) \tag{9}$$

where $V(r, \theta)$ is a steady solution of Laplace equation with non-homogeneous boundary conditions of the second kind, and $W(r, \theta, t)$ is a solution of Helmholtz equation with a homogeneous boundary of the second kind. With variables separation method applied, the general solution can be furtherly expressed as

$$T(t, r, \theta) = C_0 + D_0 \ln r + \sum_{n=1}^{\infty} \cos(2n\theta) (C_n r^{2n} + D_n r^{-2n}) + \sum_{n=1}^{\infty} \sum_{j=1}^{\infty} C_{n,j} e^{-\alpha \lambda_{n,j}^2 t} \cos(2n\theta) [C_{n,j} J_{2n}(\lambda_{n,j} r) + D_{n,j} N_{2n}(\lambda_{n,j} r)] \tag{10}$$

and the coefficients can be calculated by

$$\begin{aligned} C_0 &= T_0 - \frac{2b}{\pi} \ln a \int_0^{\frac{\pi}{2}} q_w(\theta) d\theta & D_0 &= \frac{2b}{\pi} \int_0^{\frac{\pi}{2}} q_w(\theta) d\theta \\ C_n &= \frac{2a^{-4n} \int_0^{\frac{\pi}{2}} q_w(\theta) \cos(2n\theta) d\theta}{n\pi [b^{2n-1} a^{-4n} + b^{-(2n+1)}]} & D_n &= -\frac{2 \int_0^{\frac{\pi}{2}} q_w(\theta) \cos(2n\theta) d\theta}{n\pi [b^{2n-1} a^{-4n} + b^{-(2n+1)}]} \\ C_{n,j} &= \frac{\int_a^b r \int_0^{\frac{\pi}{2}} [N'_{2n}(\lambda_{n,j} b) J_{2n}(\lambda_{n,j} r) - J'_{2n}(\lambda_{n,j} b) N_{2n}(\lambda_{n,j} r)] (T_0 - V) \cos(2n\theta) dr d\theta}{N(\lambda_{n,j}) \int_0^{\frac{\pi}{2}} \cos^2(2n\theta) d\theta} \end{aligned} \tag{11}$$

with J_n and N_n denote the Bessel functions of the first and second kinds, $\lambda_{n,j}$ denotes the j th positive eigenvalue of the n th order eigenvalue equation.

2.2. Exact solution of cylindrical concave shells

For convex case, the boundary and initial conditions can be described as:

$$T|_{r=b} = \text{const} = T_0 \tag{12}$$

$$T_\theta|_{\theta=0} = T_\theta|_{\theta=\pi/2} = 0 \tag{13}$$

$$T_r|_{r=a} = q_w(\theta) \tag{14}$$

$$T|_{t=0} = \text{const} = T_0 \tag{15}$$

Similar to the replacement of Eq. (7), Eq. (15) was replaced with $T_r|_{r=b} = 0$. For concave shells, the same form of the general solution as Eq. (10) can be derived, with different coefficients listed as follows:

$$\begin{aligned} C_0 &= T_0 - \frac{2a}{\pi} \ln b \int_0^{\frac{\pi}{2}} q_w(\theta) d\theta & D_0 &= \frac{2a}{\pi} \int_0^{\frac{\pi}{2}} q_w(\theta) d\theta \\ C_n &= -\frac{2b^{-4n} \int_0^{\frac{\pi}{2}} q_w(\theta) \cos(2n\theta) d\theta}{n\pi [a^{2n-1} b^{-4n} + a^{-(2n+1)}]} & D_n &= \frac{2 \int_0^{\frac{\pi}{2}} q_w(\theta) \cos(2n\theta) d\theta}{n\pi [a^{2n-1} b^{-4n} + a^{-(2n+1)}]} \\ C_{n,j} &= \frac{\int_a^b r \int_0^{\frac{\pi}{2}} [N_{2n}(\lambda_{n,j} b) J_{2n}(\lambda_{n,j} r) - J_{2n}(\lambda_{n,j} b) N_{2n}(\lambda_{n,j} r)] (T_0 - V) \cos(2n\theta) dr d\theta}{N(\lambda_{n,j}) \int_0^{\frac{\pi}{2}} \cos^2(2n\theta) d\theta} \end{aligned} \tag{16}$$

2.3. Approximate solution

Since the exact solution is too complex and inconvenient for application, we set up two criterions to truncate the infinite series. For the steady part $V(r, \theta)$ of single series, the criterion can be concluded that the series can be truncated when there are five consecutive terms can be neglected to the sum of previous terms. And it can be written as

$$\text{if } \left| V_{n_1} / \sum_{i=1}^n V_i \right| \leq \varepsilon, n_1 \in \{n, n + 1, n + 2, n + 3, n + 4\} \text{ then } n_1 = n \tag{17}$$

with ε set as 10^{-8} .

For the unsteady part $W(r, \theta, t)$, the truncation can be obtained in the form of two series, which were truncated over inner and outer summation. Treatment for the first summation can be written as

$$\text{for each } n, \text{ if } \left| W_{n, j_n} / \sum_{j=1}^m W_{n, j} \right| \leq \varepsilon, j_n \in \{m, m + 1, m + 2, m + 3, m + 4\} \text{ then } j_n = m \tag{18}$$

Hence, j_n might varies with n increased.

And the treatment for the second summation can be expressed as

$$\text{if } \left| \sum_{j=1}^{j_1} W_{n_2, j} / \sum_{n=1}^{n_2} \left(\sum_{j=1}^{j_1} W_{n, j} \right) \right| \leq \varepsilon, n_2 \in \{n, n + 1, n + 2, n + 3, n + 4\} \text{ then } n_2 = n \tag{19}$$

With n_1, n_2 and j_n determined respectively, the approximate solution of the temperature field can be written as

$$\begin{aligned} T(t, r, \theta) = & C_0 + D_0 \ln r + \sum_{n=1}^{n_1} \cos(2n\theta) (C_n r^{2n} + D_n r^{-2n}) \\ & + \sum_{n=1}^{n_2} \sum_{j=1}^{j_n} C_{n, j} e^{-\alpha \lambda_{n, j}^2 t} \cos(2n\theta) [C_{n, j} J_{2n}(\lambda_{n, j} r) + D_{n, j} N_{2n}(\lambda_{n, j} r)] \end{aligned} \tag{20}$$

Generally, n_1 and n_2 were less than 25, while j_n was no more than 15.

3. Numerical validations

To validate the approximate solution, numerical simulation of the transient heat conduction was carried out for the both convex and concave cases. Heat conduction equation in orthogonally curved coordinate system was adopted as the governing equation and numerical solved by Finite Difference Method. The unconditionally stable Du Fort-Frankel scheme was applied to discrete the governing equation, with second-order accuracy in both time and space [7]. The computational domain was set as $a = 3$ mm, $b = 5$ mm and $\theta \in [0, \pi/2]$, with 501 and 401 grid points uniformly distributed in r and θ direction, respectively. The material was chosen as stainless steel used in general experiment, with $\alpha = 4.29 \times 10^{-6}$ m²/s. The initial temperature was set as $T_0 = 300$ K, and boundary condition was set as $q_w(\theta) = q_0(\pi/2 - \theta)$. For both convex and concave shells, the numerical and theoretical results can match well with each other, including the temperature distribution on heated wall and temperature evolution at given position, as shown in Fig. 2. Therefore, the approximate solution was reliable for further analysis.

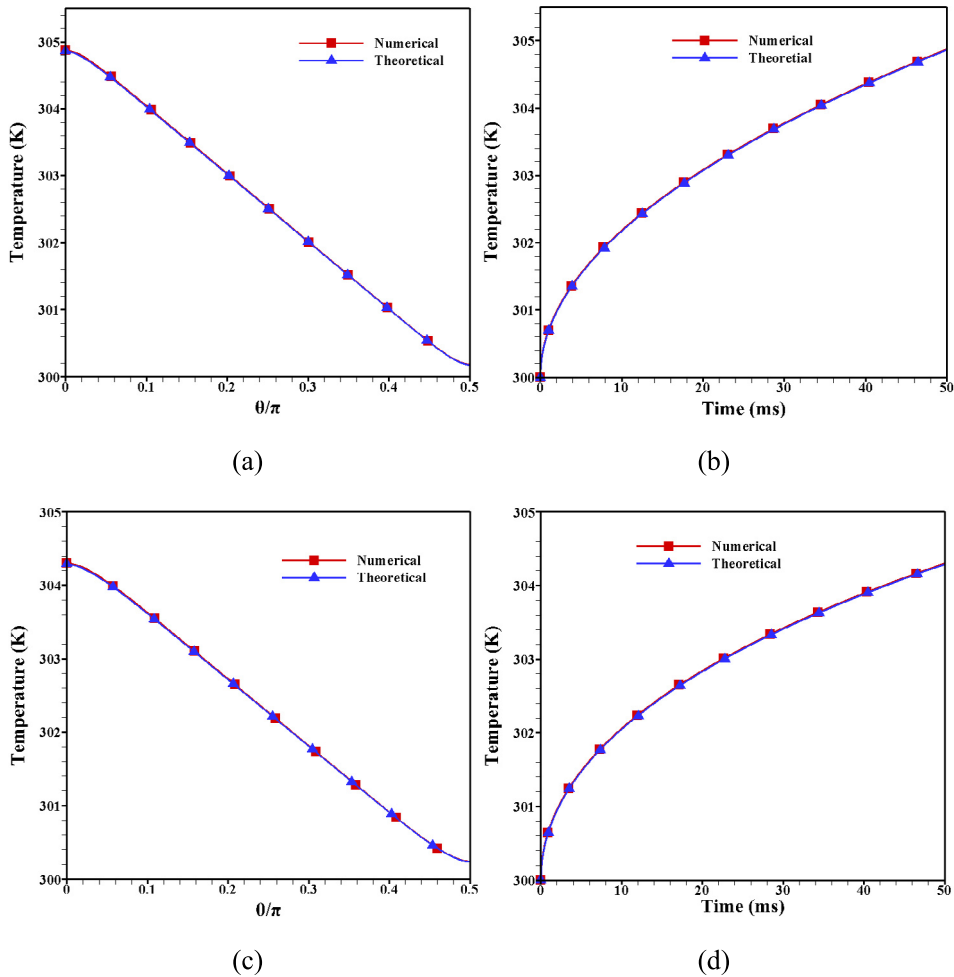


Fig. 2. Comparisons between numerical and theoretical solutions by (a) $T(r = b, t = 50 \text{ ms})$ and (b) $T(r = b, \theta = 0)$ for the convex case, and (c) $T(r = a, t = 50 \text{ ms})$ and (d) $T(r = a, \theta = 0)$ for the concave case.

4. Results and discussions

With the approximate solution Eq. (20), the temperature field in the models can be investigated analytically. To analyze the error caused by traditional one-dimensional semi-infinite theory, the temperature field at given instant and surface temperature evolution at given location were captured. The data processing for heat flux was carried out by Eq. (3) of one-dimensional theory, and compared with actual heating load. For different situation, the forms of heating load, position of heating and curvature radius were taken into considerations.

4.1. Error analysis under different forms of heating load

The solution of a cylindrically convex shell made of stainless steel was chosen for the analysis, by setting $a = 3 \text{ mm}$ and $b = 5 \text{ mm}$. Four forms of heating load were defined as $q_w(\theta) = q_0 \cos^n \theta$, with $n = 0, 1, 3, 5$ and $q_0 = 0.1 \text{ MW/m}^2$. The contour of temperature of can be directly calculated by the approximate solution, as shown in Fig. 3. Within 50 ms, the depth of heat conduction was less than 2 mm, and the boundary at $r = a$ had not been affected. The difference in distribution of temperature can be observed significantly for

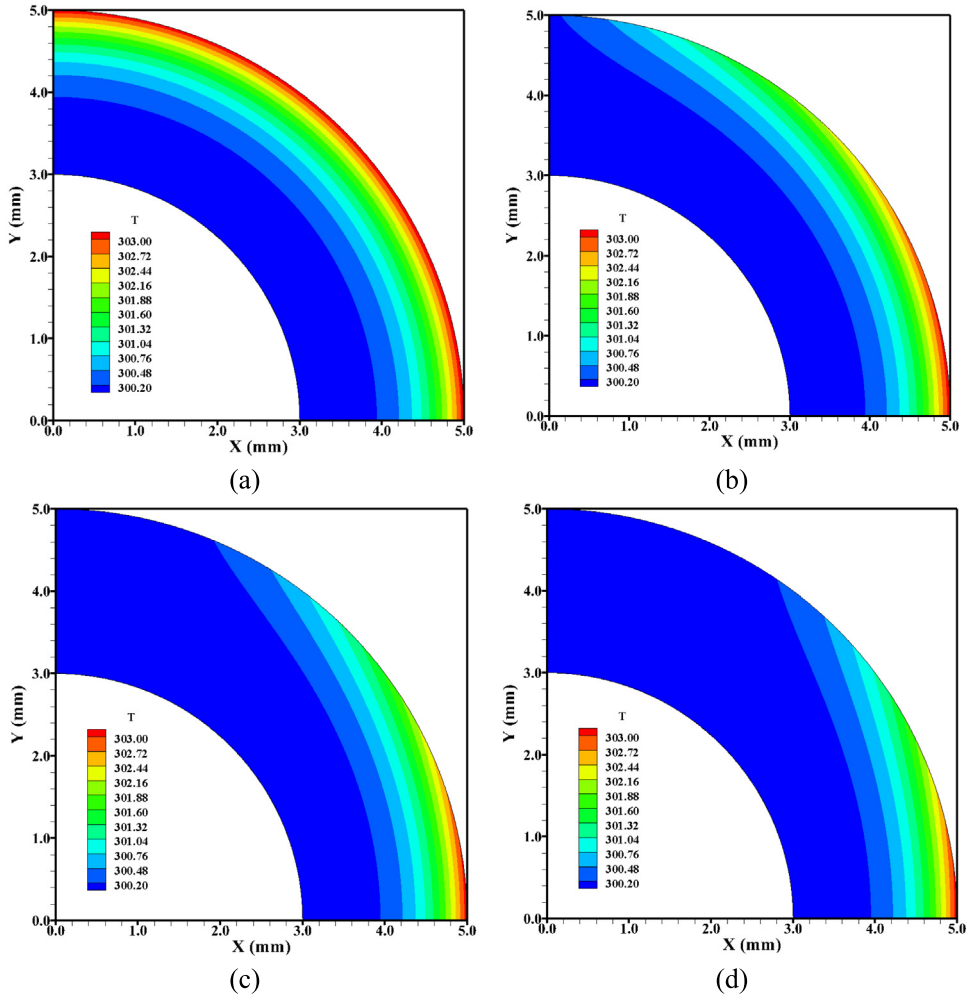


Fig. 3. Approximate solution of temperature field at 50 ms with (a) $q_w(\theta) = q_0$, (b) $q_w(\theta) = q_0 \cos \theta$, (c) $q_w(\theta) = q_0 \cos^3 \theta$ and (d) $q_w(\theta) = q_0 \cos^5 \theta$.

all the cases. For the case of $n = 0$, it is quasi one-dimensional heat conduction, the temperature distribution along θ was uniform, and the field can be described as $T(r, t)$. For cases of $n = 1, 3$ and 5 , the temperature distribution was decreased with θ increased. Hence, lateral heat conduction must play an important role for the heat flux measurement and data processing. With n increased, the heating load was more and more concentrated to the location of $(r = b, \theta = 0)$, so did the effected zones. For the later three cases, the heat fluxes in lateral direction were calculated by the approximate solution, which were as high as 10% to 15% of q_0 at 50 ms.

The data processing for the heat flux at $(r = b, \theta = 0)$ was operated by Eq. (3), and compared with q_0 , as shown in Fig. 4. At 50 ms, the error was estimated to be 5.6% to 3.2%, and decreased with n increased. And the reason was due to the decrease of effected zones, which had been mentioned before. Therefore, it might be regarded as a hint for us that larger effected zone came by larger data processing error. It was different from the traditional knowledge for the measurement and data processing under concentrated heating load at some components of vehicles caused by complex flows and interactions.

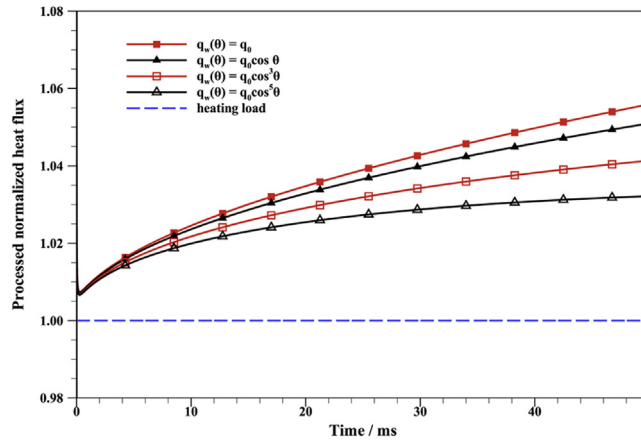


Fig. 4. Processed heat flux by one-dimensional theory at $(r = b, \theta = 0)$ for convex shells.

4.2. Error analysis with different heating surface and curvatures

As mentioned in former sections, the scale of effected zone of heat conduction significantly influences the data processing error. If the local curvature radius decreased, the effected zone will be relatively increased. Therefore, the local curvature radius of aircraft components must obviously affect the error of processed heat flux. And both convex and concave shells were investigated by different curvature radius for the effect to error, which can also be named as local scale effect. For convex shells, five geometrical configurations were designed for analysis, with curvature radius b decreased from 5.0 mm to 3.0 mm; and for concave shells, five geometrical configurations were designed with curvature radius a decreased from 3.0 mm to 1.0 mm. In all ten cases, the wall thickness $(b - a)$ was always kept a constant as 2.0 mm. And the heating load form of $q_w(\theta) = q_0$ and $q_0 = 0.1 \text{ MW/m}^2$ was applied as the boundary condition at $r = b$ for convex cases and $r = a$ for concave cases, respectively.

The processed heat fluxes by Eq. (3) and their evolutions over time were indicated in Fig. 5(a). For convex cases, the processed heat fluxes were about 5.1% to 8.2% higher than the actual value of q_0 . Since the heat was transferred in the direction from $r = b$ to $r = a$, the space for the heat was compressed, which made the processed heat flux higher. In contrast, the heat fluxes were about 8.9% to 25.8% lower than the actual q_0 in concave cases. Due to the space expanded from $r = a$ to $r = b$, processed heat flux was lower than actual value. Interestingly, with the decrease of the curvature radius for both convex and concave cases, the relative error between processed heat flux and q_0 will increased significantly. The nonlinear distribution of $|\text{error}|$ can be consider as evidence for the scale effect caused by local curvature radius, as shown in Fig. 5(b).

5. Conclusions

In this paper, approximate solutions for both cylindrically convex and concave shells were established, truncating the infinite series of exact solutions. The validations of the approximate solutions were carried out by numerical simulations. The approximate solutions were applied to analyze the error for the heat flux processing by traditional one-dimensional semi-infinite theory, with different forms of heating load, position and local curvature radius of heated surface taken into consideration. With observations and comparisons of results, it found that the error increased with effected zone of heat conduction relatively increased. Especially for decrease of local curvature radius, the scale effect significantly and nonlinearly increased errors during measurement and data processing for heat flux.

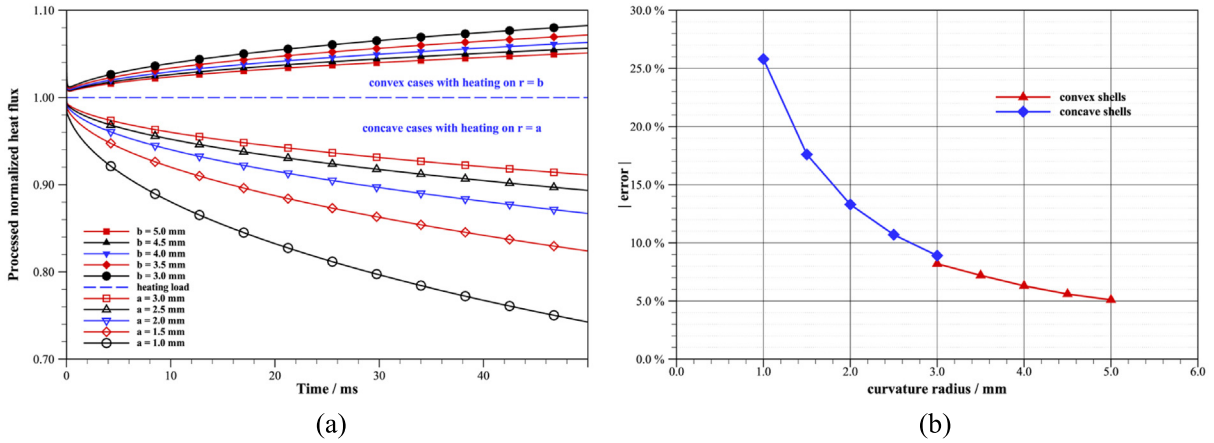


Fig. 5. (a) Processed heat flux by one-dimensional theory and evolution over time with different local curvature radius at $\theta = 0$; (b) absolute value of processed heat flux error varied with curvature radius at $t = 50$ ms.

Acknowledgments

This work was supported by the National Key Research and Development Program of China (2019YFA0405204) and National Natural Science Foundation of China (12132017, 11872066 and 11727901).

References

- [1] D. Walker, E. Scott, Evaluation of estimation methods for high unsteady heat fluxes from surface measurements, *J. Thermophys. Heat Transfer* 12 (1998) 543–551.
- [2] B. Hollis, S. Borrelli, Aerothermodynamics of blunt body entry vehicles, *Prog. Aerosp. Sci.* 48-49 (2012) 42–56.
- [3] Y. Liu, Y. Mitsutake, M. Monde, Development of fast response heat transfer measurement technique with thin-film thermocouples, *Int. J. Heat Mass Transfer* 162 (2020) 120331.
- [4] S. Agarwal, N. Sahoo, R. Singh, Experimental techniques for thermal product determination of coaxial surface junction thermocouples during short duration transient measurements, *Int. J. Heat Mass Transfer* 103 (2016) 327–335.
- [5] V. Tulovsky, L. Papiez, Formula for the fundamental solution of the heat equation on the sphere, *Appl. Math. Lett.* 14 (2001) 881–884.
- [6] G. Han, Z. Jiang, Approximate analytic solution of heat conduction in hollow semi-spheres flying at hypersonic speed, *Int. Commun. Heat Mass Transfer* 43 (2013) 46–52.
- [7] E. Du Fort, S. Frankel, Stability conditions in the numerical treatment of parabolic differential equations, *Math. Tables Aids Comp.* 7 (1953) 135–152.